Electronic Supplementary Information

Ring opening polymerization of lactides and lactones by multimetallic alkyl zinc complexes derived from the acids $Ph_2C(X)CO_2H$ (X = OH, NH_2)

Yahya F. Al-Khafaji,[a] Mark R.J. Elsegood,[b] Josef W. A. Frese [b] and Carl Redshaw*[a]

[a] *Department of Chemistry, The University of Hull, Cottingham Rd, Hull, HU6 7RX, U.K.*

[b] *Chemistry Department, Loughborough University, Loughborough, Leicestershire, LE11 3TU, U.K.*

E-mail: C.Redshaw@hull.ac.uk

Contents

Ring opening polymerisation

Table S1. Optimum condition screening for the ROP of ε-CL, *rac*-LA and δ-VL using **4**.

For ε-CL

Figure S10. Relationship between [ε-CL]/[**4**] and the number of average molecular weight and PDI of the polymer.

Figure S11. ^{1}H NMR spectrum of polycaprolactone (run 1 table 1).

Figure S12. ^{13}C NMR spectrum of polycaprolactone (run 1 table 1).

Figure S13. MALDI-ToF spectrum of PCL (run 8, table S1).

For rac-LA

Figure S14. Relationship between [*rac*-LA]/[**4**] and the number of average molecular weight and PDI of the polymer.

Figure S15. ^{1}H NMR spectrum of polylactide (run 6 table 1).

Figure S16. ^{13}C NMR spectrum of polylactide (run 6 table 1).

Figure **S17**. MALDI-ToF spectrum of PLA (run 6, table 1).

Figure S18. Homonuclear decoupled ^{1}H NMR spectrum of of PLA (run 6, table 1).

Figure S19. 2D J-resolved ^{1}H NMR spectrum of PLA (run 6, table 1).

Figure S20. Homonuclear decoupled ^{1}H NMR spectrum of PLA (run 8, table 1).

Figure S21. 2D J-resolved ^{1}H NMR spectrum of PLA (run 8, table 1).

For δ-VL

Figure S22. Relationship between [δ-VL]/[**4**] and the number of average molecular weight and PDI of the polymer.

Figure S23. ^{1}H NMR spectrum of PVL (run 11 table 1).

Co-polymerization of ε-CL and rac-LA.

Figure S24. ^{1}H NMR spectrum of copolymer PCL+ PLA, table 2 run 1.

Figure S25. ^{13}C NMR spectrum of co-polymer PCL+ PLA, table 2 run 1.

Figure S26. DSC plot of co-polymer from ε-CL and *rac*-LA, table 2 run 2.

Chart S1. Previously reported metal/main group complexes derived from 2,2′-diphenylglycine.

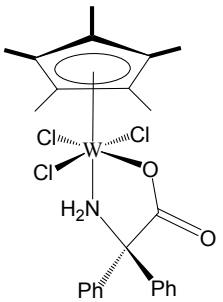

Redshaw 1997

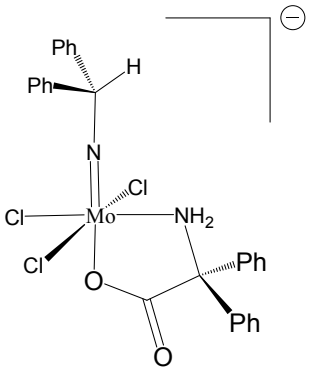

Gibson 1997

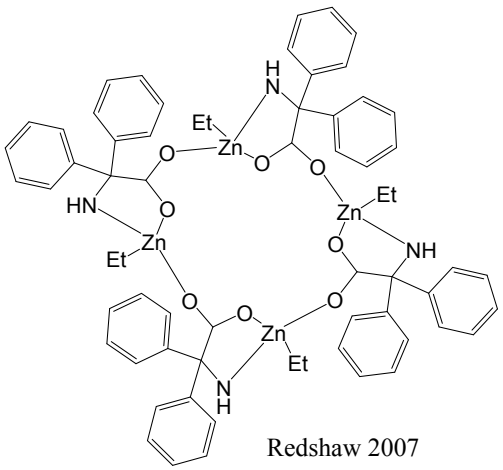

Redshaw 2007

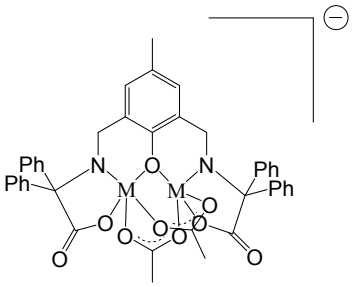

Redshaw 2011 (M= Cu, Zn)

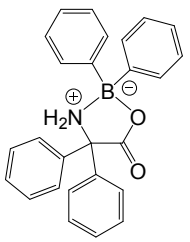

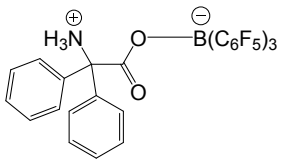

Redshaw 2009

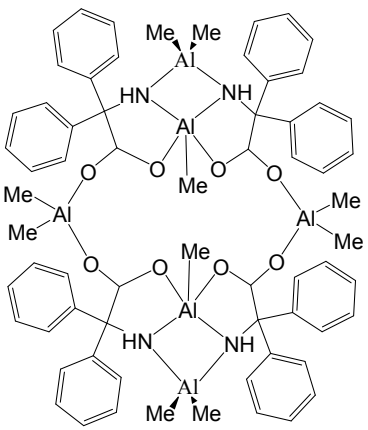

Redshaw 2005

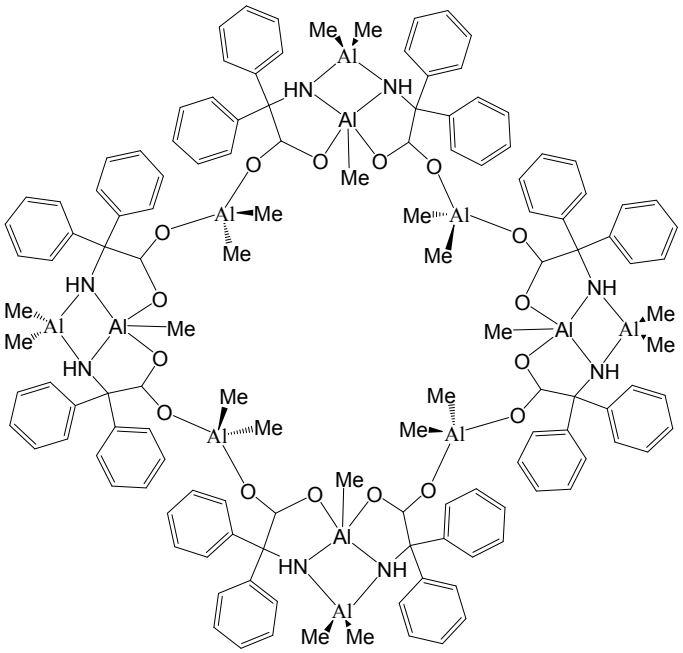

Redshaw 2005

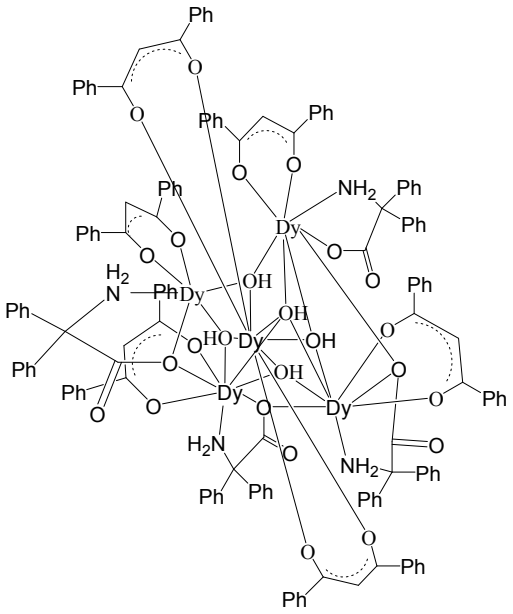

Powell, Roesky 2013

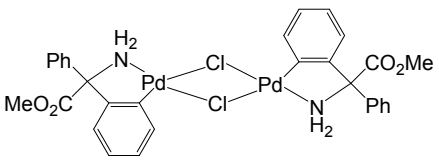

Martinez, Urriolabeitia 2013

References

[1] C. Redshaw, V. C. Gibson, W. Clegg, A. J. Edwards and B. Miles, *J. Chem. Soc. Dalton Trans*. 1997, 3343.
[2] V. C. Gibson, C. Redshaw, W. Clegg and M. R. J. Elsegood, *J. Chem. Soc. Dalton Trans*. 1997, 3207.
[3] C. Redshaw and M. R. J. Elsegood, *Angew. Chem. Int. Ed*. 2007, **46**, 7453.
[4] C. Redshaw, M. R. J. Elsegood and K. E. Holmes *Angew. Chem. Int. Ed*. 2005, **44**, 1884.
[5] A. Arbaoui, C. Redshaw, D. L. Hughes and M. R. J. Elsegood, *Inorg. Chimica Acta*. 2009, **362**, 509.
[6] A. Arbaoui, C. Redshaw, N. M. Sanchez-Ballester, M. R. J. Elsegood and D. L. Hughes, *Inorg. Chimica Acta*, 2011, **365**, 96.
[7] E. Laga, A. Garcia-Montero, F. J. Sayago, T. Soler, S.Moncho, C. Cativiela, M. Martinez, E. P. Urriolabeitia, *Chem.-Eur.J.*2013 ,**19**,17398
[8] D. T. Thielemann, A. T. Wagner, Y. Lan, C. E. Anson, M. T. Gamer, A. K. Powell, P. W. Roesky, *Dalton Trans. ,*2013, **42**, 14794

Crystallography

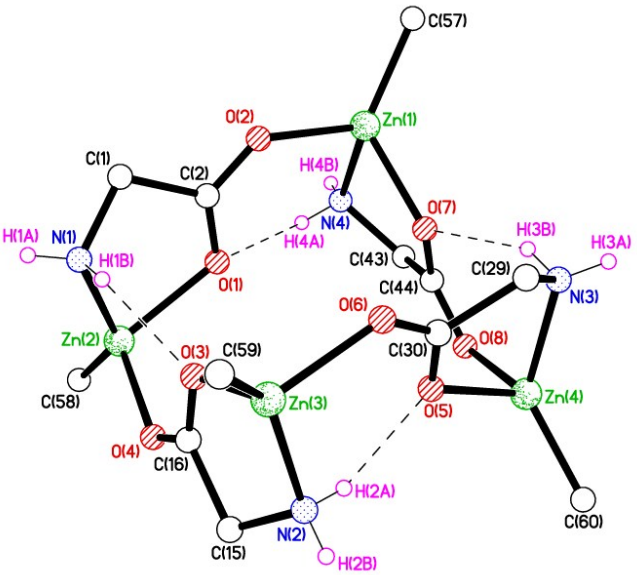

Figure S1. Alternative view of **1**.

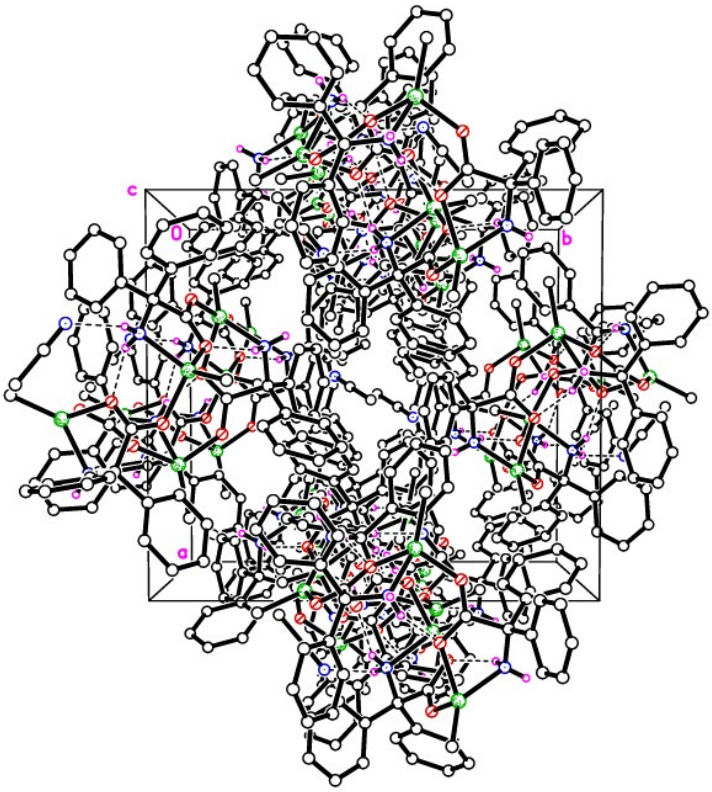

Figure S2. Packing diagram of **1**.

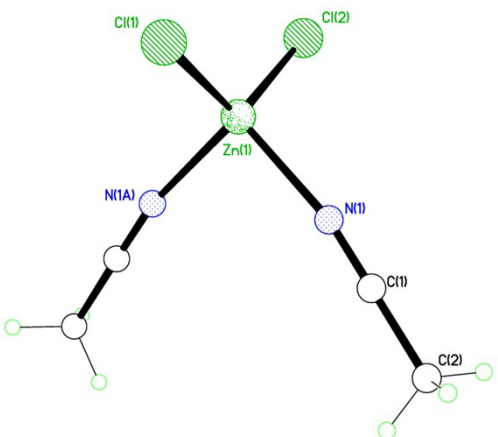

Figure S3. View of $[ZnCl_2(NCMe)_2]$

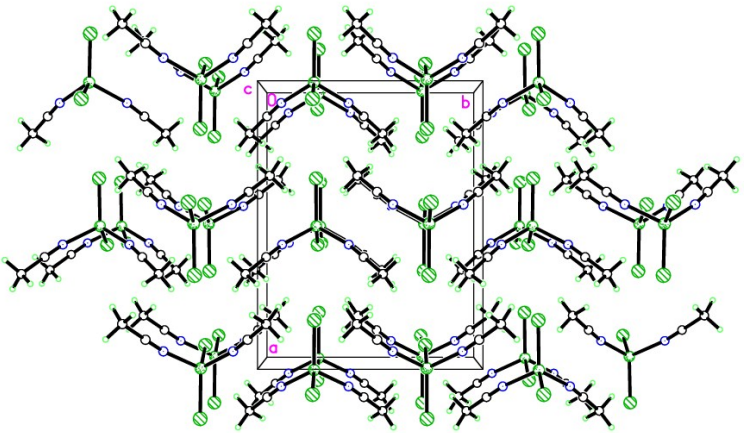

Figure S4. Layered structure in $[ZnCl_2(NCMe)_2]$

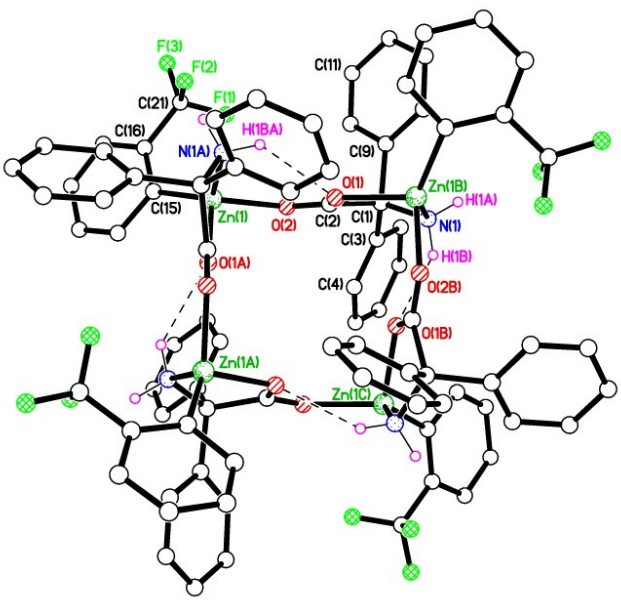

Figure S5. Alternative view of **3**.

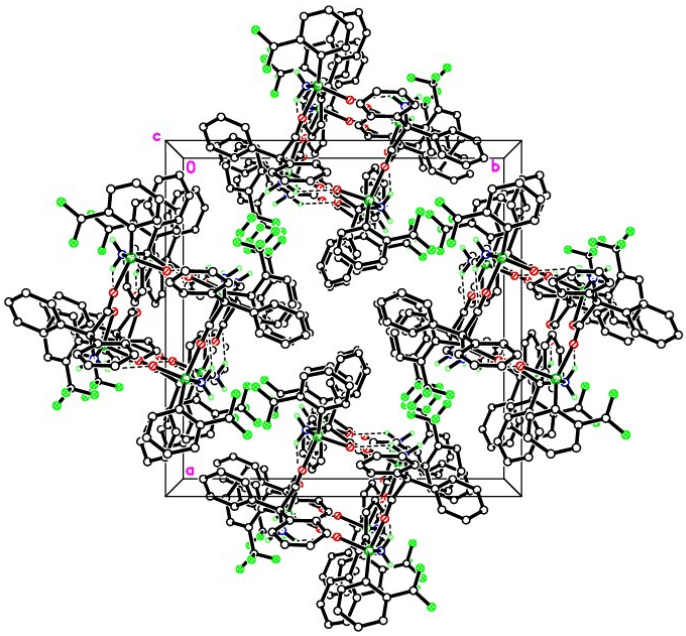

Figure S6. Packing diagram for **3**.

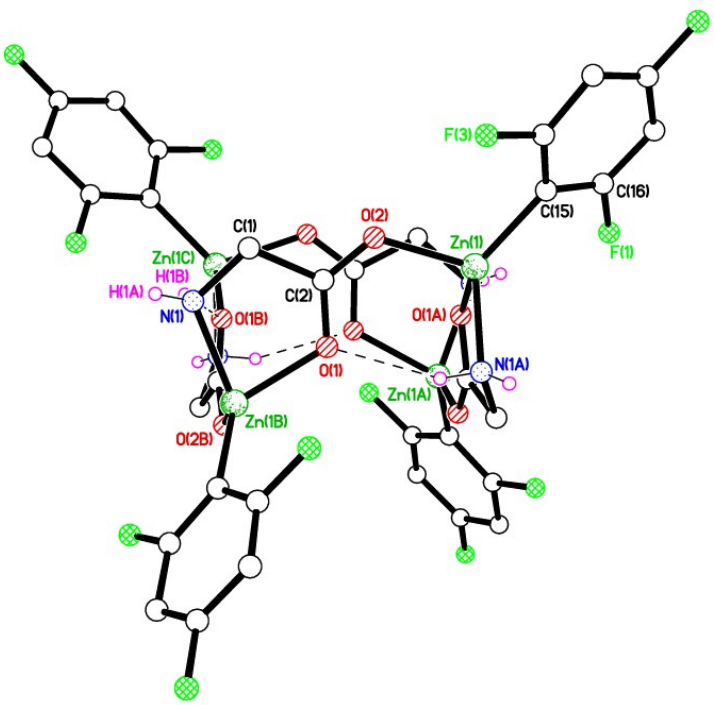

Figure S7. Alternative view of **4**.

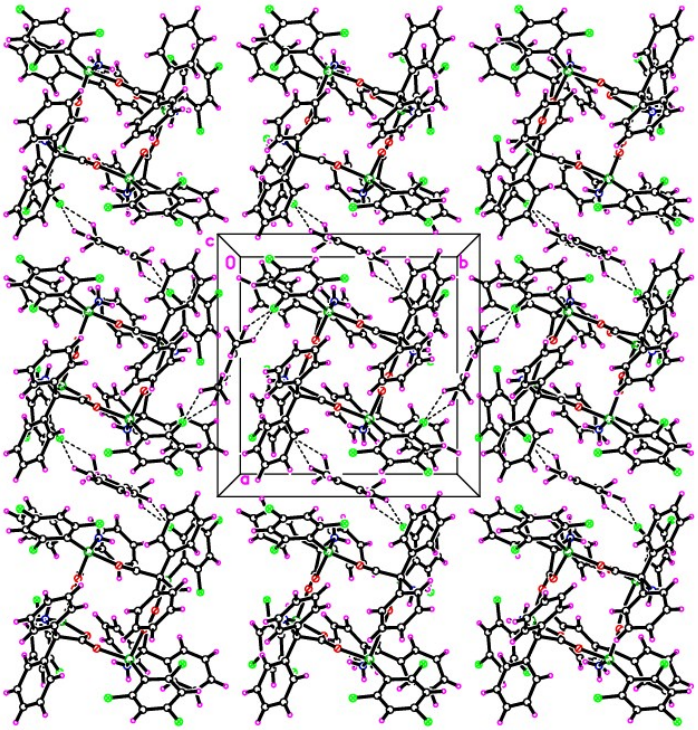

Figure S8. Packing diagram of **4**.

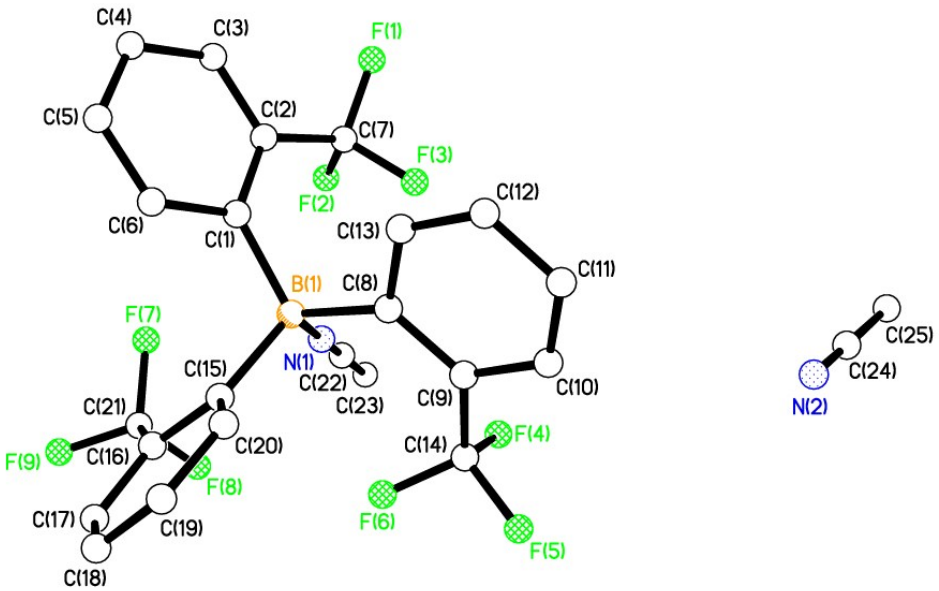

Figure S9. Molecular structure of $(2\text{-}CF_3C_6H_4)_3B(NCMe)\cdot MeCN$. Selected bond lengths (Å) and angles (°): B(1) – N(1) 1.5857(17), B(1) – C(1) 1.6507(19), B(1) – C(8) 1.6450(19), B(1) – C(15) 1.6434(19); N(1) – B(1) – C(1) 107.58(10), N(1) – B(1) – C(8) 106.65(10), N(1) – B(1) – C(15) 108.31(10).

Ring opening polymerisation

Table S1. Optimum condition screening for the ROP of ε-CL, *r*-LA and δ-VL using **4**.

Run	Monomer	[Monomer]:[Cat]:[OH]	Time/h	Temp/°C	Conv[a] (%)	M_n[b]$\times 10^3$,GPC	$M_{n,Cal}$[c]	PDI[d]
1	ε-CL	125:1:0	1	110	91	11400	12980	1.40
2	ε-CL	250:1:0	1	110	78	15000	22260	1.38
3	ε-CL	375:1:0	1	110	88	20800	37670	1.41
4	ε-CL	500:1:0	1	110	91	33700	51930	1.68
5	ε-CL	625:1:0	1	110	85	43800	60640	1.43
6	ε-CL	750:1:0	1	110	89	56200	76190	1.51
7	ε-CL	250:1:0	3	80	69	8590	19690	1.21
8	ε-CL	250:1:0	3	60	22	3850	6280	1.09
9	ε-CL	250:1:0	3	25	---	---	---	---
10	ε-CL	250:1:1	1	110	67	2580	19230	1.10
11	*r*-LA	50:1:0	12	110	74	3370	5330	1.19
12	*r*-LA	100:1:0	12	110	67	6150	9660	1.23
13	*r*-LA	150:1:0	12	110	61	9670	13190	1.27
14	*r*-LA	200:1:0	12	110	65	13000	18740	1.51
15	*r*-LA	250:1:0	12	110	60	15400	21620	1.37
16	*r*-LA	300:1:0	12	110	64	22900	27670	1.40
17	*r*-LA	150:1:0	12	80	19	1460	4110	1.09
18	δ-VL	50:1:0	24	110	42	860	2100	1.04
19	δ-VL	100:1:0	24	110	58	2670	5810	1.13
20	δ-VL	150:1:0	24	110	41	3210	6160	1.23
21	δ-VL	200:1:0	24	110	31	4750	6210	1.08
22	δ-VL	250:1:0	24	110	51	5800	12770	1.25
23	δ-VL	300:1:0	24	110	60	8820	18020	1.12

[a] Determined by ^{1}H NMR spectroscopy; [b] Calculated from $([Monomer]_0/[Cat]_0) \times$ conv.(%) × Monomer molecular weight; [c] M_n from GPC. [d] From GPC.

Figure S10. Relationship between [CL]/[**4**] and the number of average molecular weight and PDI of the polymer.

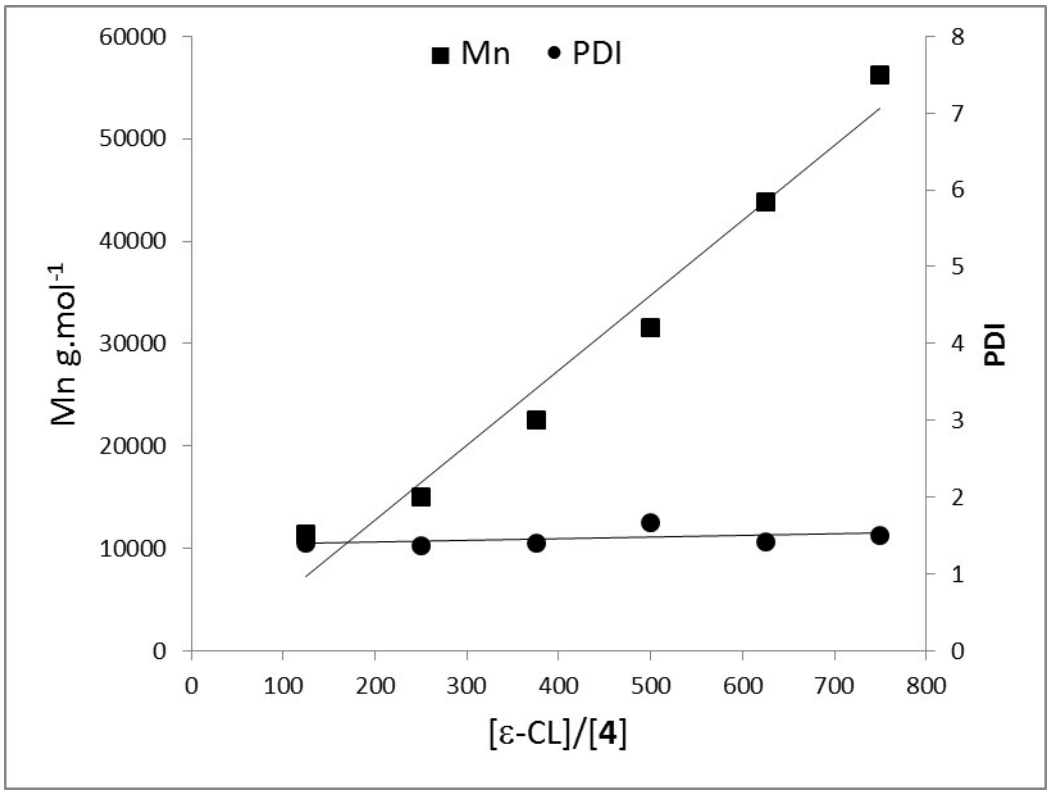

Figure S11. ^{1}H NMR spectrum of polycaprolactone (run 1 table 1).

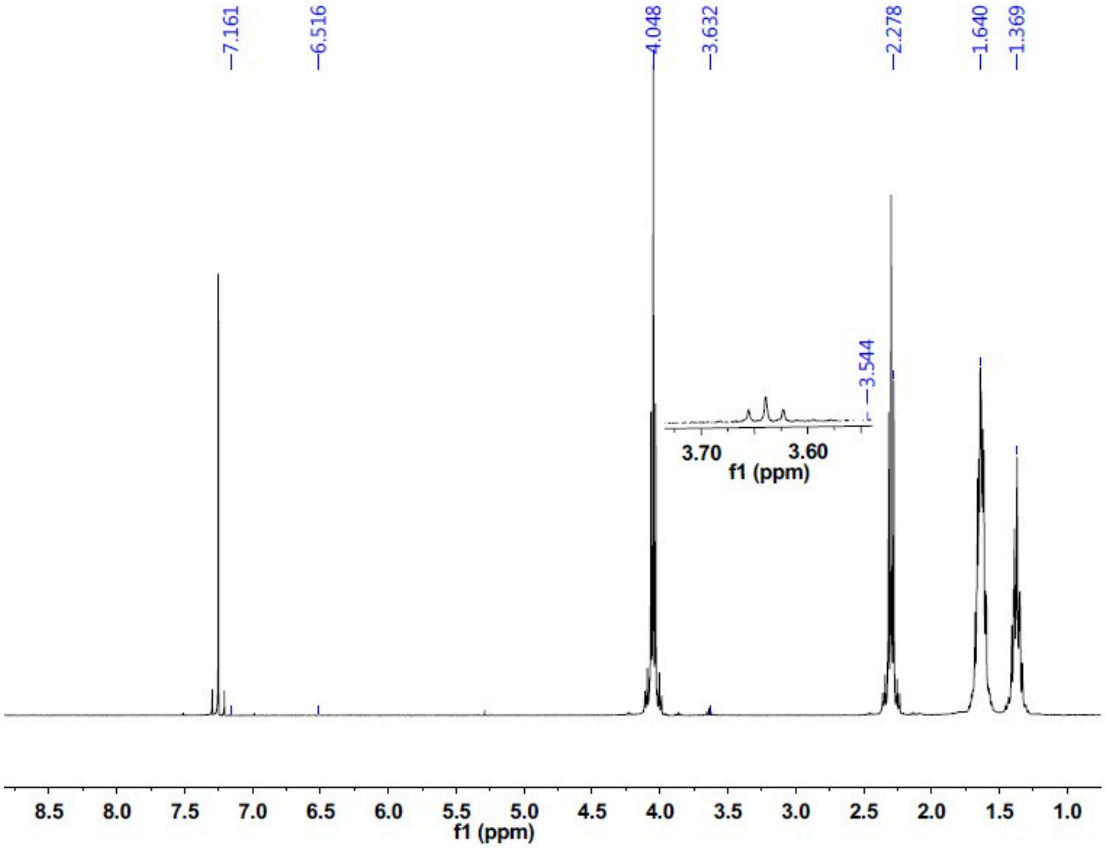

Figure S12. ^{13}C NMR spectrum of polycaprolactone (run 1 table 1).

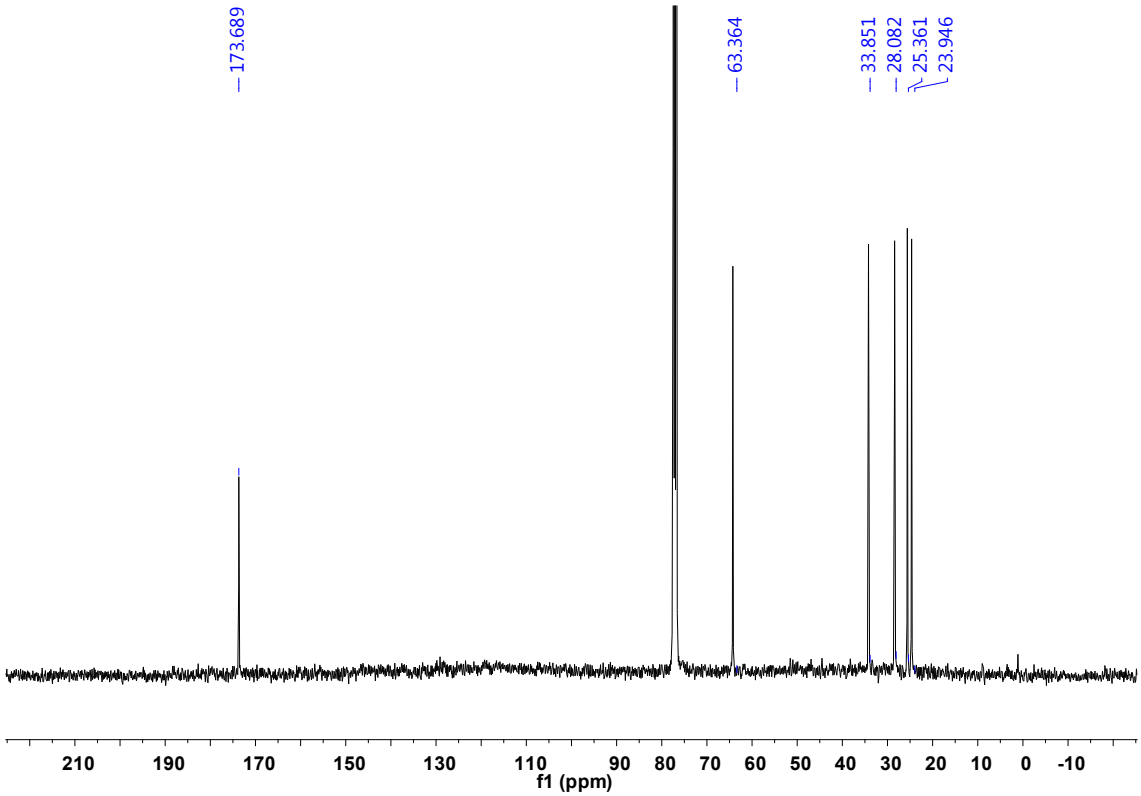

Figure S13. MALDI-ToF spectrum of PCL (run 8, table S1).

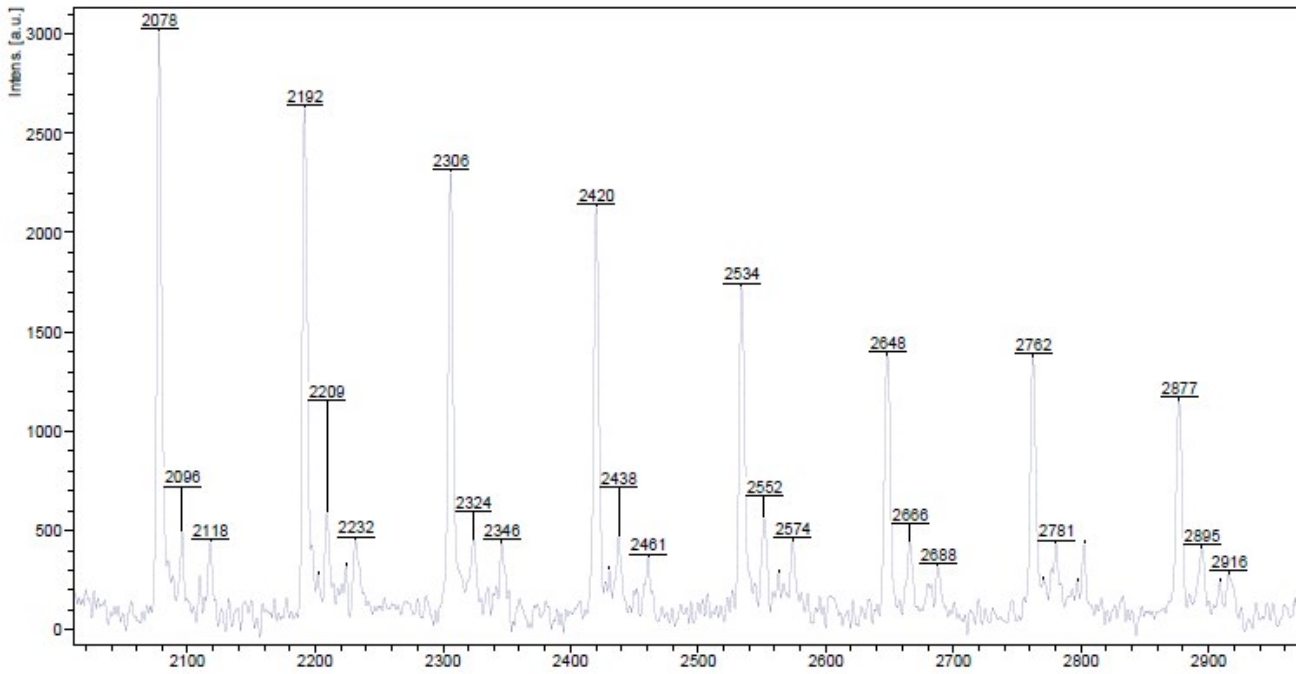

Figure S14. Relationship between [*rac*-Lactide]/[**4**] and the number of average molecular weight and PDI of the polymer.

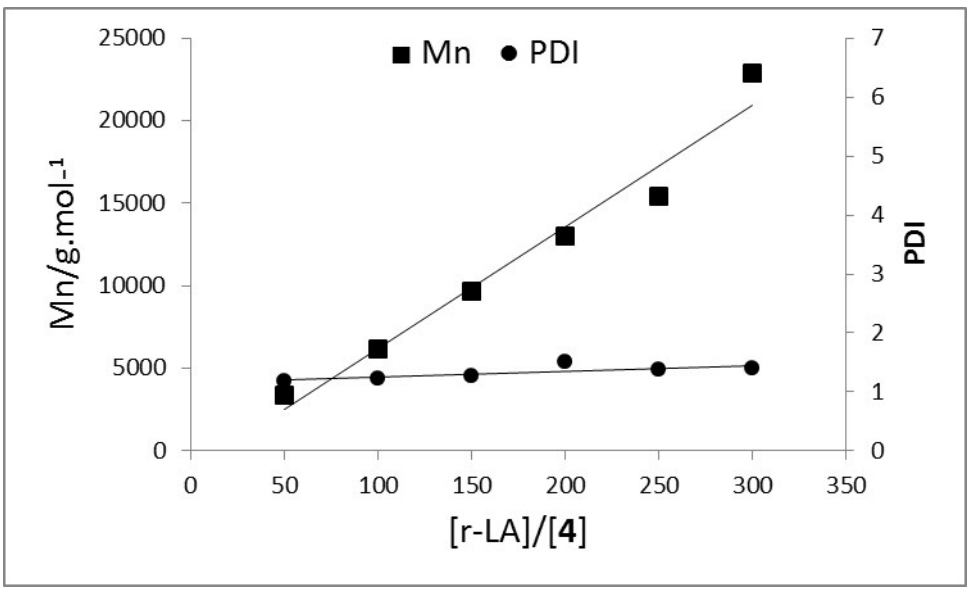

Figure S15. ^{1}H NMR spectrum of polylactide (run 6 table 1).

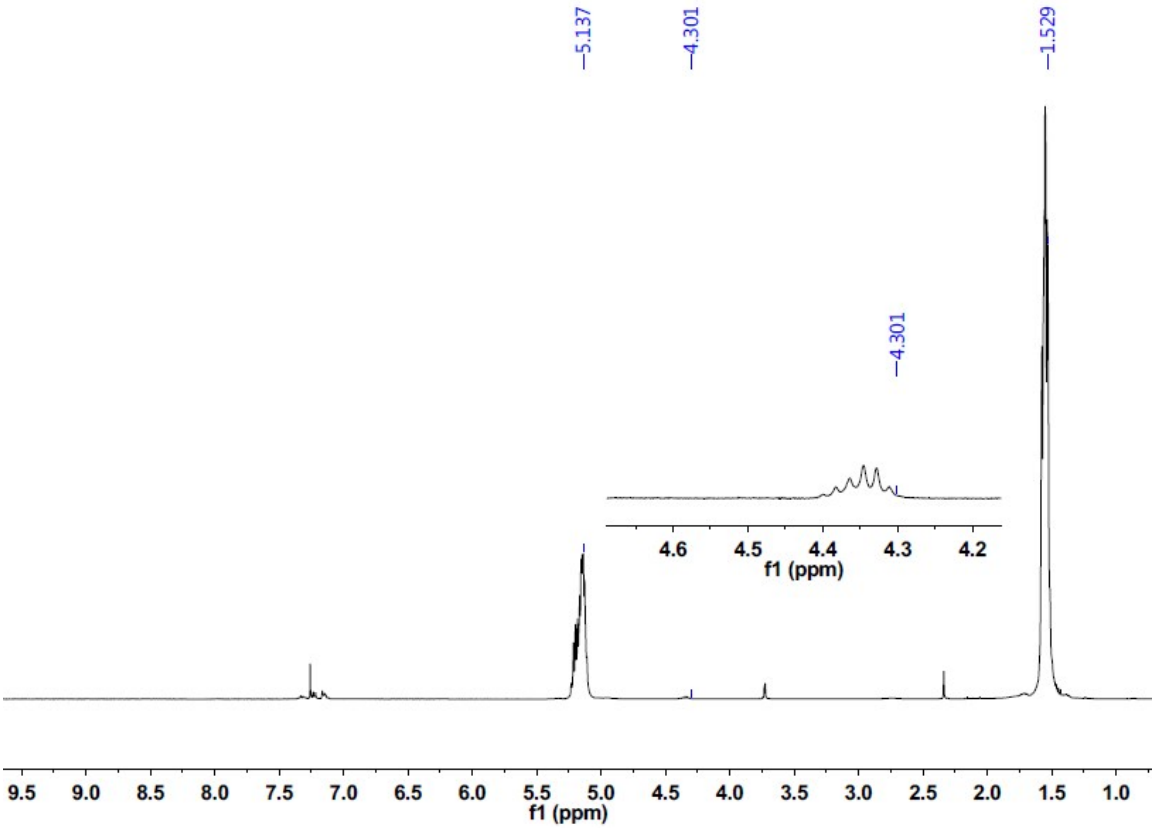

Figure S16. ^{13}C NMR spectrum of polylactide (run 6 table 1).

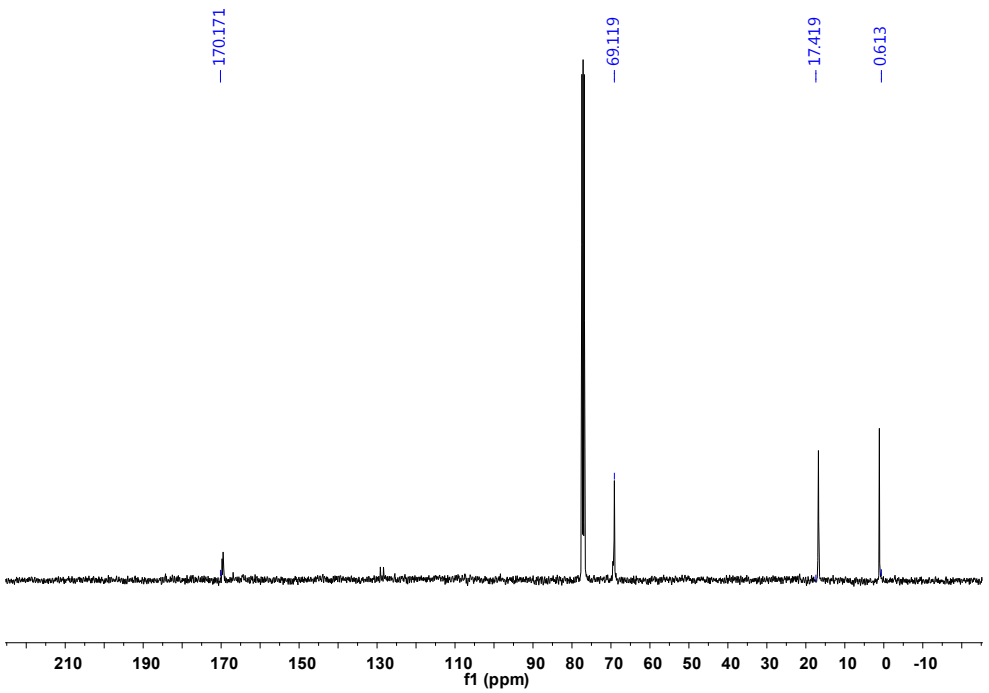

Figure S17. MALDI-ToF spectrum of poly(*r*ac-LA) (run 6, table 1).

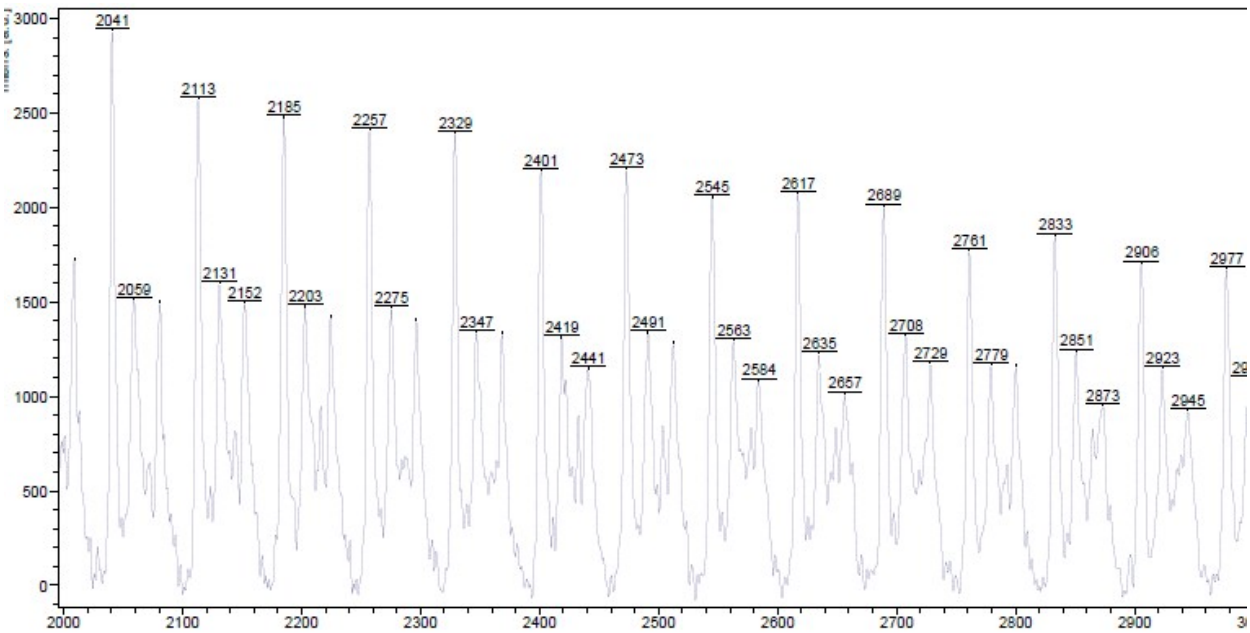

Figure S18. Homonuclear decoupled ^{1}H NMR spectrum of of poly(*r*-LA), (run 6, table 1).

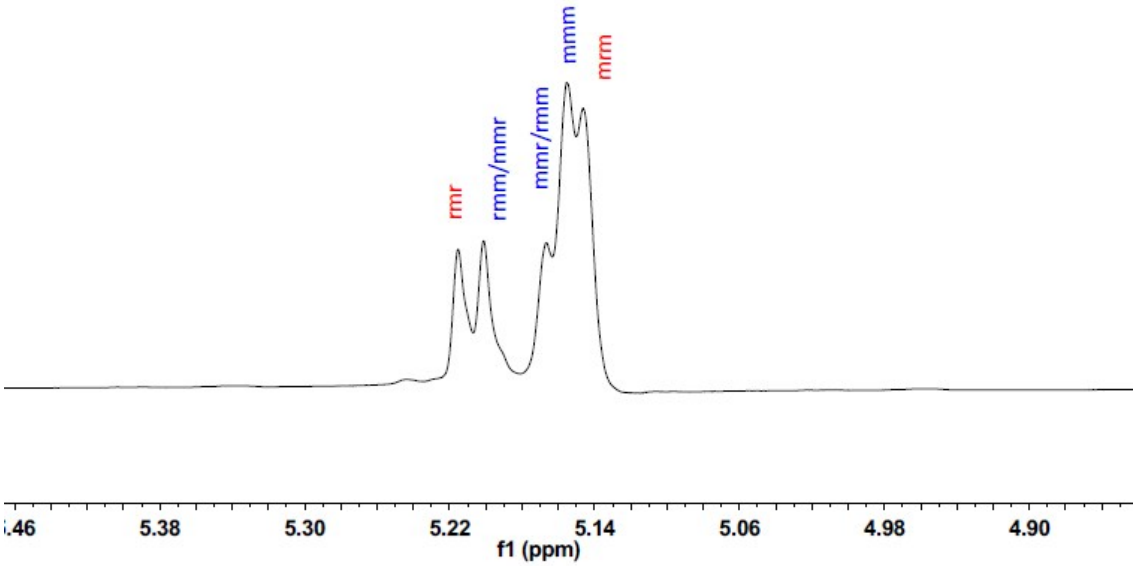

Figure S19. 2D J-resolved ^{1}H NMR spectrum of poly(*r*-LA) (run 6, table 1).

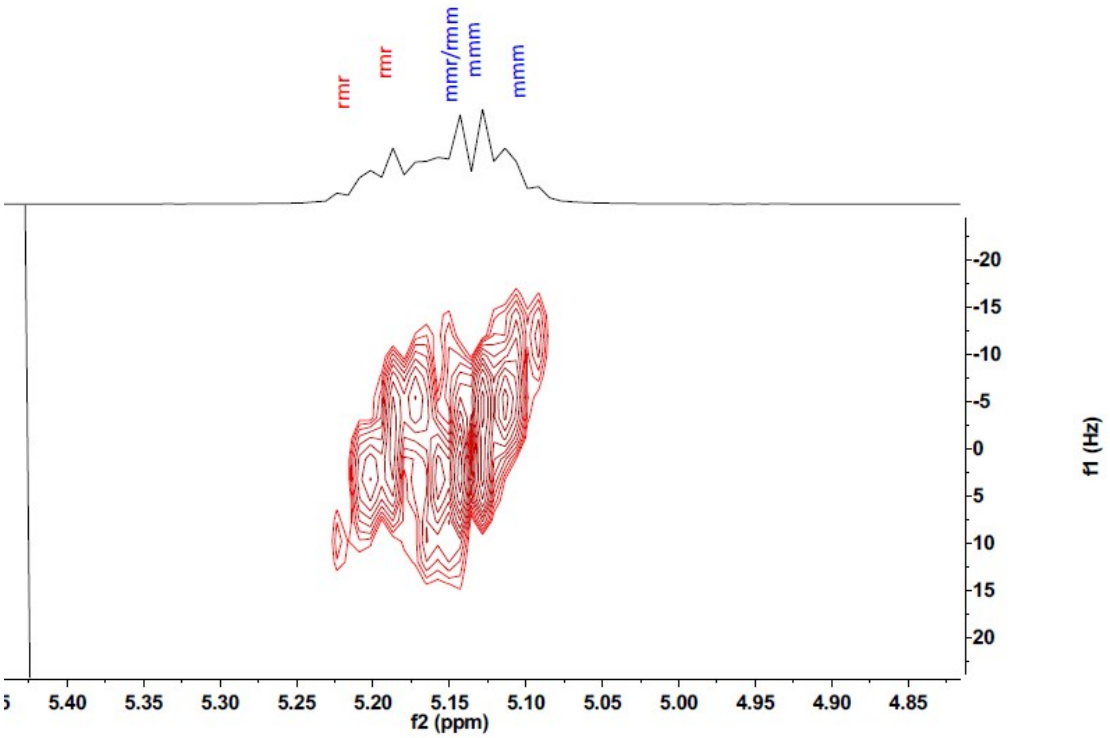

Figure S20. Homonuclear decoupled ^{1}H NMR spectrum of of poly(*r*-LA), (run 8, table 1).

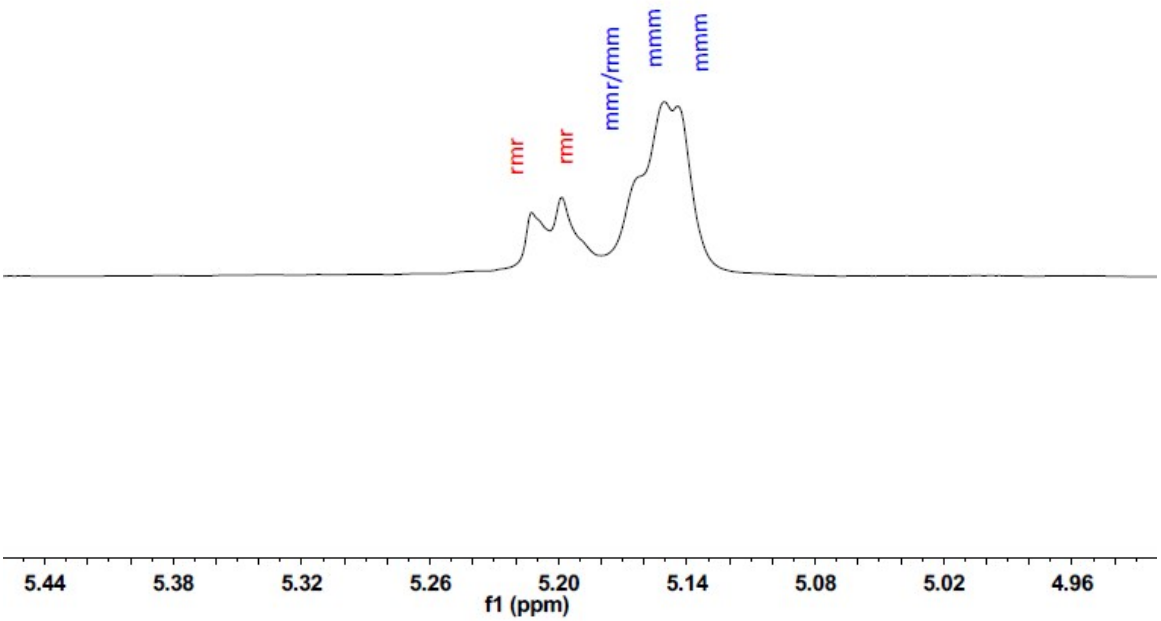

Figure S21. 2D J-resolved ^{1}H NMR spectrum of poly(*r*-LA) (run 8, table 1).

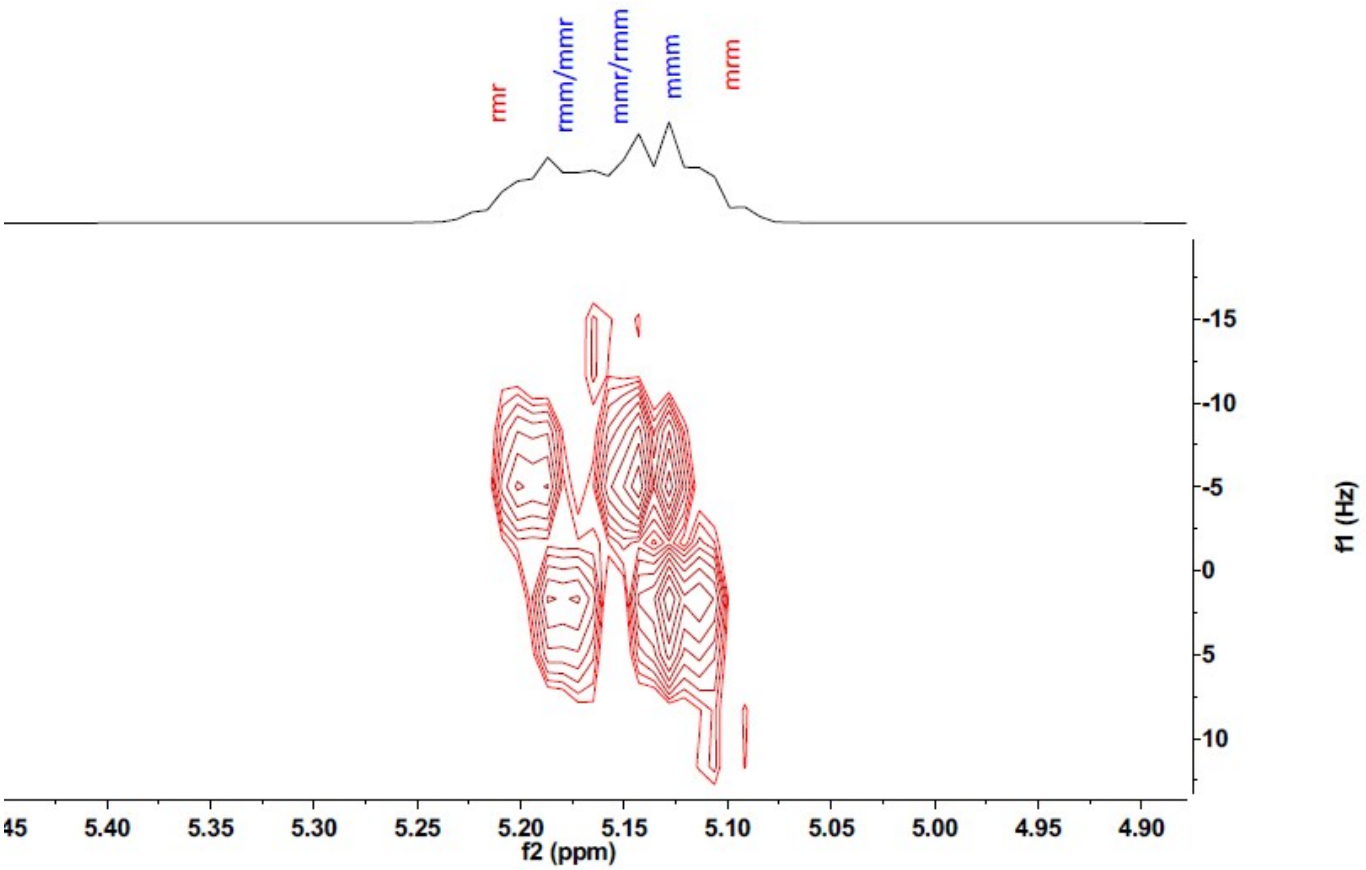

Figure S22. Relationship between [δ-VL]/[**4**] and the number of average molecular weight and PDI of the polymer.

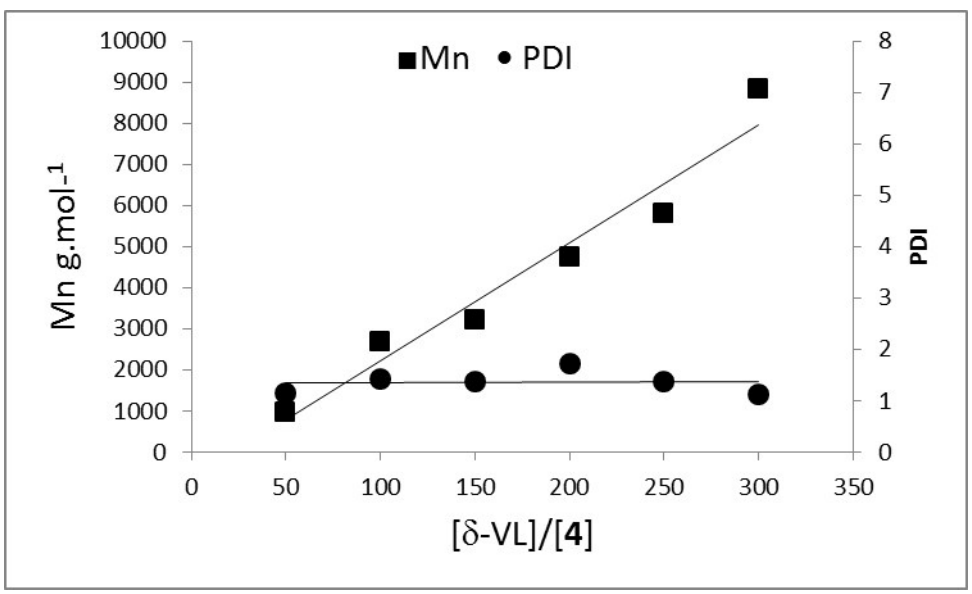

Figure S23. ^{1}H NMR spectrum of PVL (run 11 table 1).

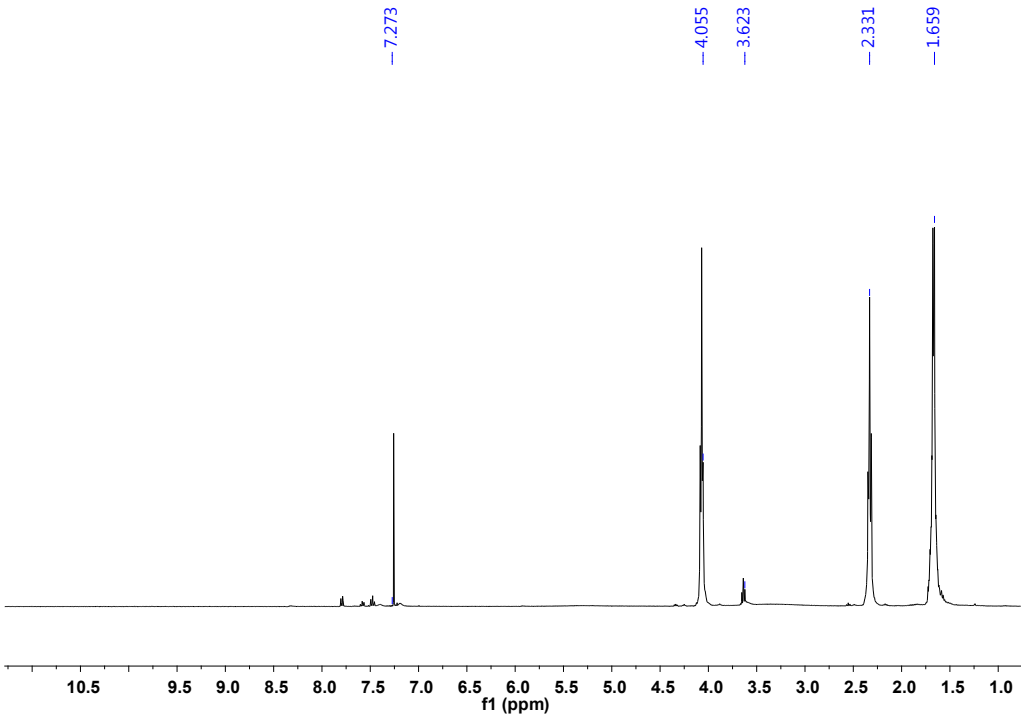

Figure S24. ^{1}H NMR spectrum of copolymer PCL+ poly(*r*-LA), table 3 run 1.

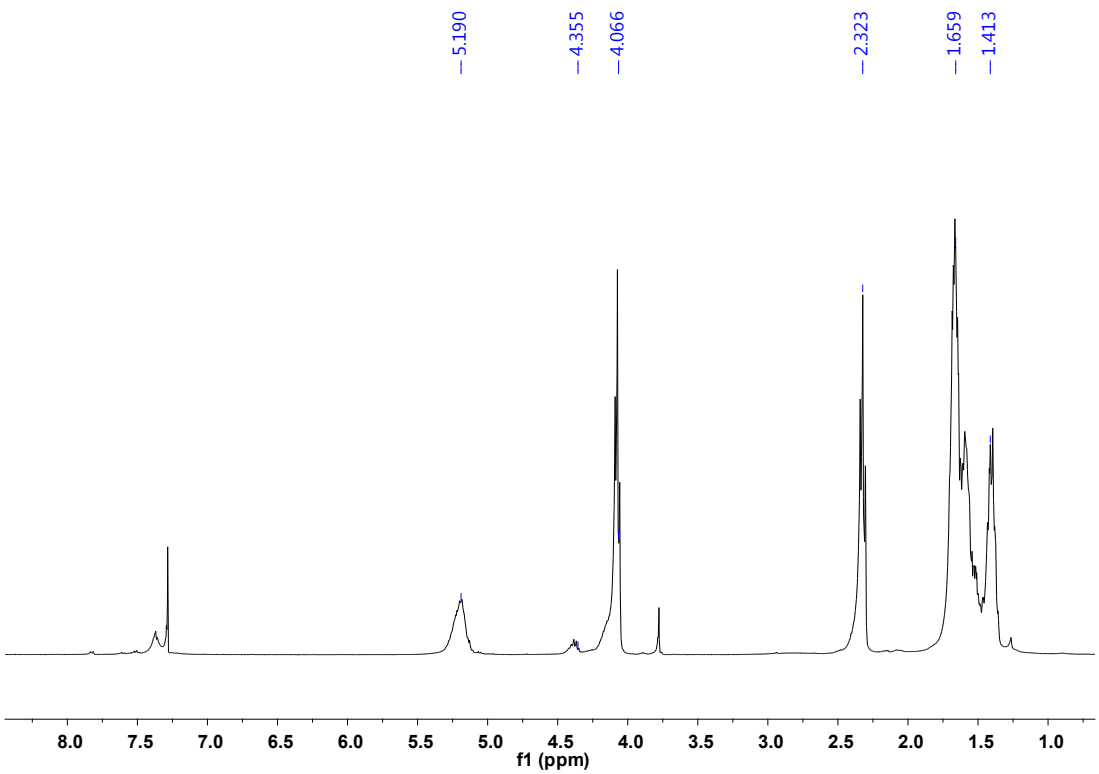

Figure S25. ^{13}C NMR spectrum of co-polymer PCL+ PLA, table 3 run 7.

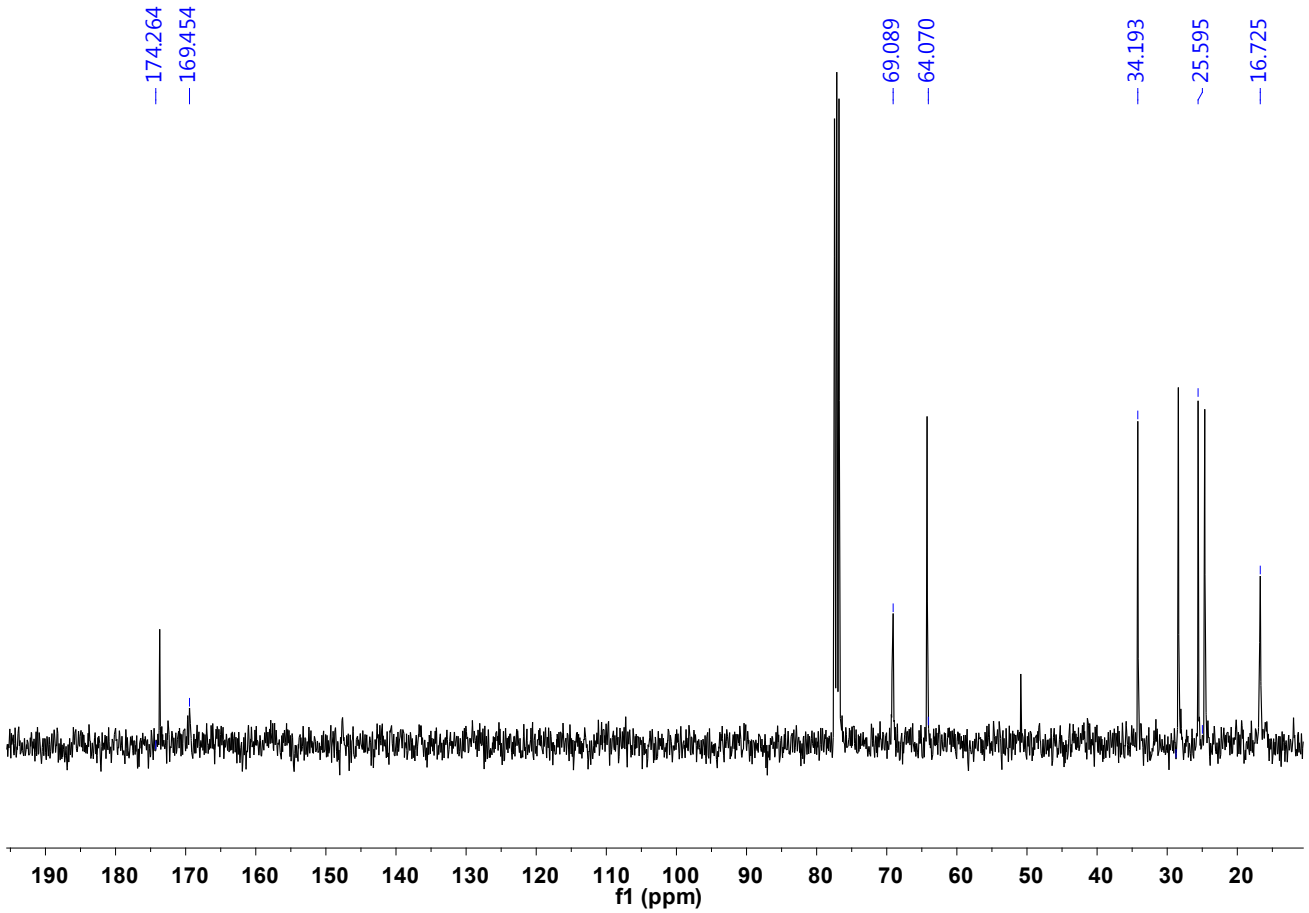

Figure S26. DSC plot of co-polymer from ε-CL and *rac*-LA, table 2 run 2.